Proceedings of NAWTEC16
16th Annual North American Waste-to-Energy Conference
May 19-21, 2008, Philadelphia, Pennsylvania, USA

NAWTEC16-1916

The effects of varied hydrogen chloride gas concentrations on corrosion rates of commercial tube alloys under simulated environment of WTE facilities

Shang-Hsiu Lee and Marco J. Castaldi

Department of Earth & Environmental Engineering (HKSM)
Columbia University, New York, NY 10027

ABSTRACT

In order to clarify the effects of HCl concentrations on corrosion rates of commercial tubing in Waste-to-Energy (WTE) boilers, a corrosion test was made by altering the HCl concentration from 0 to 1000ppm, together with simulated flue gas composition. Three commercial tubing SA178A, SA213 T11 and NSSER-4 samples were investigated under a well controlled thermal gradient where the gas temperature was at 700^0C and metal temperatures ranged from 480 to 580^0C. The duration of each test was 100 hours. The post-test analyses included observations of surface morphology and elementary composition analysis of corrosion products by scanning electron microscope (SEM) and energy dispersive spectroscopy (EDS). The corrosion rates were acquired by measuring the mass loss of samples after the test.

The results showed that the addition of HCl to the flue gas increased the corrosion rates of test samples, but the relation between the HCl concentration and corrosion rate was not linear. The HCl effects on corrosion rates were more prominent when its concentration changed from 0 to 500ppm. In addition, the HCl effects were promoted by the increase of metal temperature in particular when metal temperature was over 560^0C.

INTORDUCTION

Chlorine induced high temperature corrosion that degrades the boiler tubes has long been a major issue of maintaining the Waste-to-Energy (WTE) facilities. The difficulty of combating corrosion problem in WTE facilities is that it varies from unit to unit and is highly related to the composition of feed and the boiler design. Municipal Solid Wastes (MSW) typically consists of paper, plastics, leather, wood, glass, metals and food waste. During combustion, nearly all of the chlorine content in the various components of the MSW, both natural organics and chlorinated plastics is volatilized and converted to hydrogen chloride gas. In the U.S. MSW contains about 0.5% of chlorine [1], and the hydrogen chloride gas concentration in the flue gas is calculated to be about 580 ppmv [2]. The practical concentrations of hydrogen chloride gas in WTE facilities vary during the operation because of the heterogeneous nature of the feed.

Laboratory investigations on the corrosion behavior have been performed in chlorine-containing atmospheres with different

temperatures on several metals and alloys [3-6]. Most of these studies have shown that even small changes of the oxygen/chlorine ratio or temperature can influence the corrosion behavior. A recent in-situ study indicates that significantly increased corrosion rate was observed when extra chlorine in the form of PVC was added to the fuel mix [7]. It is generally accepted that the mechanisms of chlorine induced "active oxidation" occurs at metal temperature above 450^0C and comprises several steps: (a) the formation of chlorine at the scale surface, (b) penetration of chlorine into the scale to the oxide/metal interface, (c) formation of metal chlorides on the metal surface, (d) diffusion of metal chlorides outwards through the crack and pores of the scale, and (e) reaction of metal chloride with available oxygen in the atmosphere to produce metal oxide and chlorine [6, 8].

In the authors' previous laboratory research, an apparatus which can create a controlled thermal gradient between synthetic flue gas and metal surface has been modified to examine the corrosion rates of different commercial steels under simulated combustion atmosphere in WTE facilities. The obtained corrosion rates have reflected the annual wastages of boiler tubes in WTEs [9]. The present research aims to compare and quantify the corrosion rates of three wildly used commercial steels by altering the concentration of hydrogen chloride gas in the synthetic flue gas.

EXPERIMENTAL PROCEDURE

Three commercial steels, SA178A, SA213-T11 and NSSER-4 were tested in this research. SA178A and SA213-T11 have been widely used as the base tube of superheater. NSSER-4 is developed by a Japanese steel company which claims its good resistance to chlorine corrosion. The chemical compositions of these three steels are summarized in Table 1. All steels were cut to dimensions of 1"×1"×0.08" by a water–cooled machine. The preparation of samples followed the ASTM standard which included grinding with 120-grit SiC paper, degreasing with acetone in ultrasonic baths and drying at 100 ^{0}C for one hour. After that the clean, dry samples were measured and weighted.

Corrosion tests were carried out in a furnace at the gas temperature of 700^0C for 100 hours. The furnace had a constant temperature zone of about 13 inches for exposing the test samples. A sample carrier made of a square stainless steel tube was placed in the furnace. Cooling air was passed through the sample carrier to extract the heat from the surface of it. A schematic cross-section of the furnace and the sample carrier is shown as Fig. 1. The sample carrier had six reliefs to place samples and each was equipped with a thermocouple to monitor the sample temperature. The sample temperature was controlled by the flow rate of cooling air through the tubular passage, thus inducing the desired thermal gradient between outer flue gas flow and metal surface.

Table 1. Chemical composition (wt. %) of test samples

Steel	C	Si	Mn	P	S	Ni	Cr	Mo	Fe	Nb+Ta	Others
SA178A	0.07	0.06	0.47	0.01	0.004	0.054	0.016	0.01	bal.	0.002	Cu=0.119 Al=0.026 Ca=0.001 N=0.008 Ti=0.003 V=0.002
SA213-T11	0.08	0.28	0.43	0.014	0.002	-	1.05	0.52	bal.		
NSSER-4	0.04	2.5	0.8	-	-	13.1	17.3	2.5	bal.		

During the 100-hour test, each sample was maintained at stable temperature. By controlling the flow rate of the cooling air, surface temperatures of six samples were controlled within the range of 480-580^{0}C, and the thermal gradient (under furnace temperature of 700^{0}C) was controlled from 120-240^{0}C. This setup enabled a single test to yield five plots of temperature versus time, with one duplicate set for comparison.

The composition of synthetic flue gas in the test consisted of 8% O_2, 12% CO_2, 0-1000ppmv HCl, 100ppmv SO_2, 15% water vapor, and balanced with N_2 at a total gas flow rate of 500 ml/min. The gas was preheated up to 250 ^{0}C before being injected into the furnace.

After the tests, samples were cooled down in the furnace and prepared for subsequent corrosion product analyses, metallographic corrosion rate observations, and mass loss corrosion rate measurement. Analyses of the surface morphology and elementary composition of the corrosion product were conducted by using a scanning electron microscope (SEM) equipped with an energy dispersive spectroscopy (EDS) unit.

The measurement of mass loss corrosion rate followed the ASTM standard. A cleaning cycle that combined procedures of light brushing, ultrasonic cleaning, chemical cleaning, and mass loss measurement was repeated several times until the corrosion products were removed completely. Final sample weights were measured to the nearest 0.001 g and adjusted for blank weight losses in the cleaning process. Corrosion rates for the bare samples were converted using mass loss, exposed area, density, and test duration.

RESULTS and DISCUSSIONS

1. SA178A

Figure 2a is the image of the sample after the 100 hrs test with metal temperature of 560^{0}C and non HCl-containing gases. A very thin scale was developed on the metal surface. The SEM image (Fig. 2b) shows that the scale was very porous and consisted of petaline shape oxide. The elementary analysis by EDS indicated that the surface of the scale was rich in Fe and O with small amounts of S (Fig. 2c). The finding by SEM and EDS, together with thermodynamic calculation indicated the oxides were mainly Fe_2O_3.

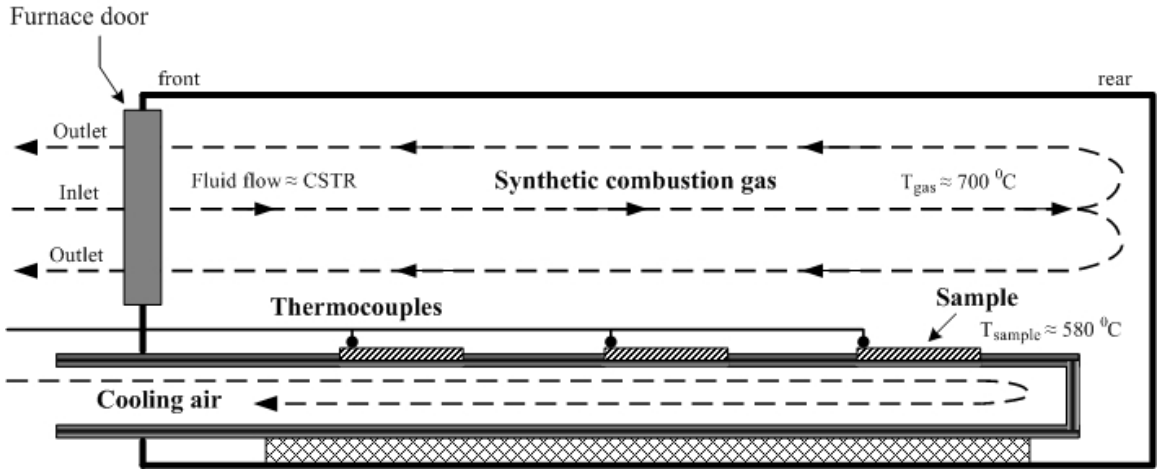

Fig. 1 The schematic cross-section of the furnace and sample carrier

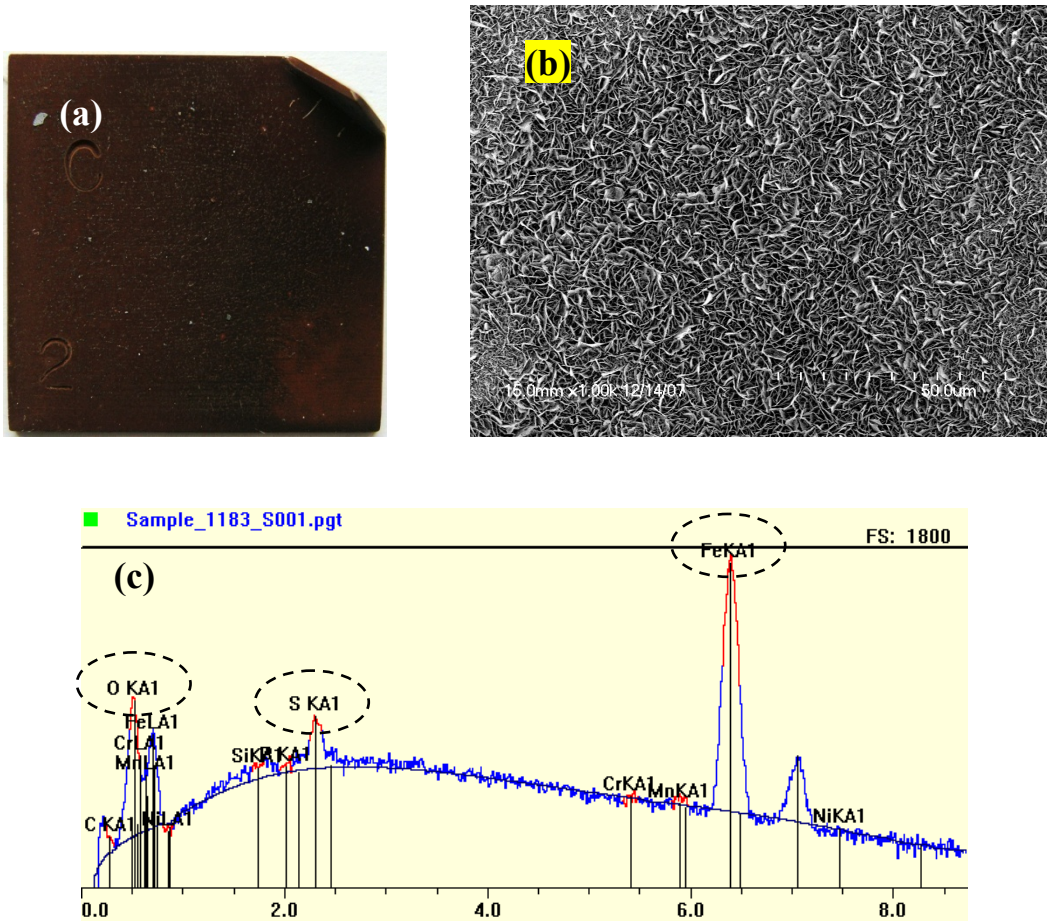

Fig. 2 (a) Surface morphology of sample SA178A tested with non HCl-containing gases, (b) SEM images of the scale, and (c) Elementary analysis of the scale

Figure 3a is the SEM image of the scale/metal interface (metal temperature of 517^0C and non HCl-containing gases) whose original scale was removed for examination. The scale/metal interface showed a porous grain structure. EDS results which identified high Fe and S concentrations with very low O content inferred the buildup of $FeS_2/Fe_2S_3/FeS$ on the scale/metal interface (Fig 3b).

Figure 4a is the image of the sample after the 100 hrs test with metal temperature of 560^0C and 1000ppm HCl-containing gases. This sample was more corroded if compared to the sample without HCl-containing gases treatment. The black-reddish scale was thicker and suffered from severe spallation when cooled down. The SEM image (Fig. 4b) also shows porous, petaline shape oxide on the scale, but unlike the previous sample the scale had high S content except Fe and O (Fig. 4c). In an oxidizing atmosphere the thermodynamic stability of metal chlorides, metal sulfate and oxides at a given temperature depends on the partial pressures of O_2, Cl_2 and SO_2. The thermodynamic phase stability diagrams for the system Fe-O_2-Cl_2 and Fe-O_2-SO_2 at 560^0C are shown as Fig. 5a and 5b in which the equilibrium conditions of the test were marked. According to these diagrams the scale consisted of Fe_2O_3 and $Fe_2(SO_4)_3$ which was consistent with the findings from EDS.

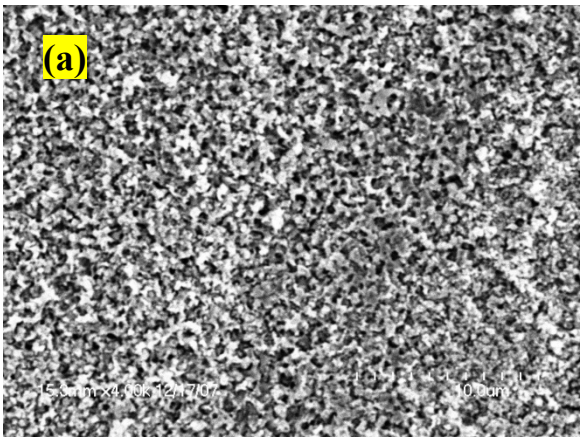

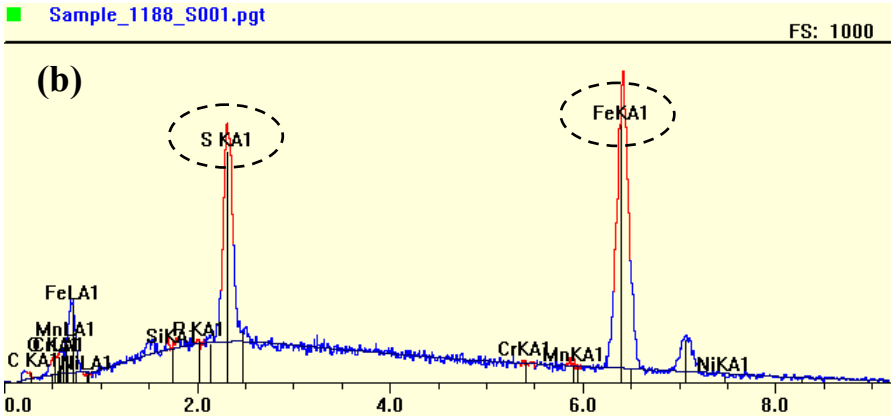

Fig. 3 (a) SEM images of the base metal after removal of scale, and (b) Elementary analysis of the scale/metal interface

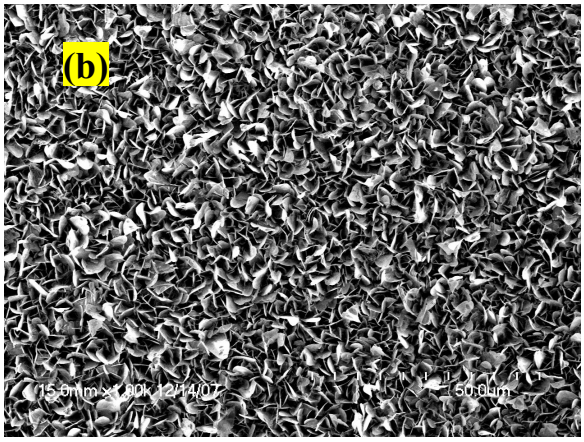

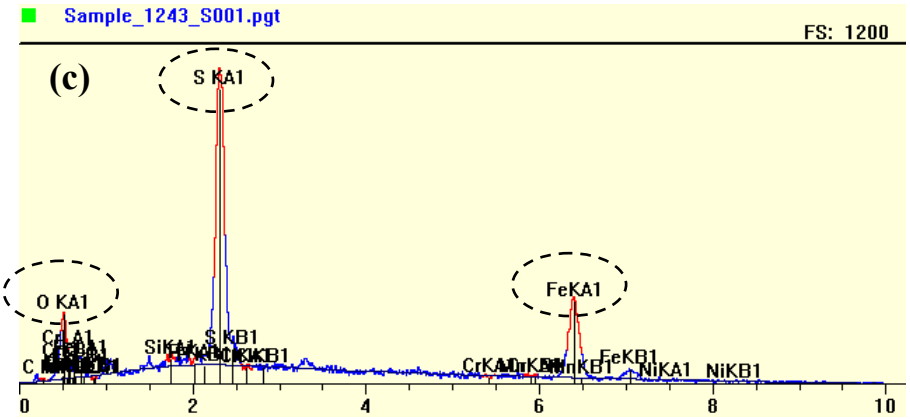

Fig. 4 (a) Surface morphology of sample SA178A tested with 1000ppm HCl-containing gases, (b) SEM images of the scale, and (c) Elementary analysis of the scale

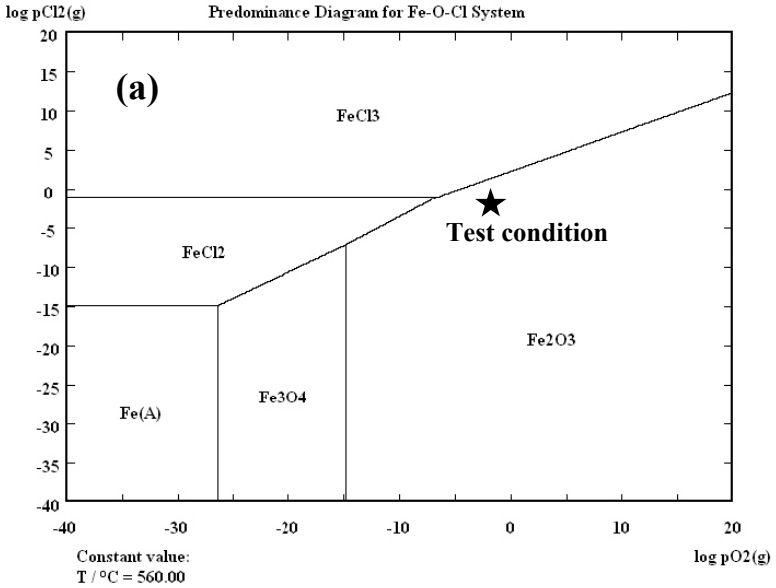

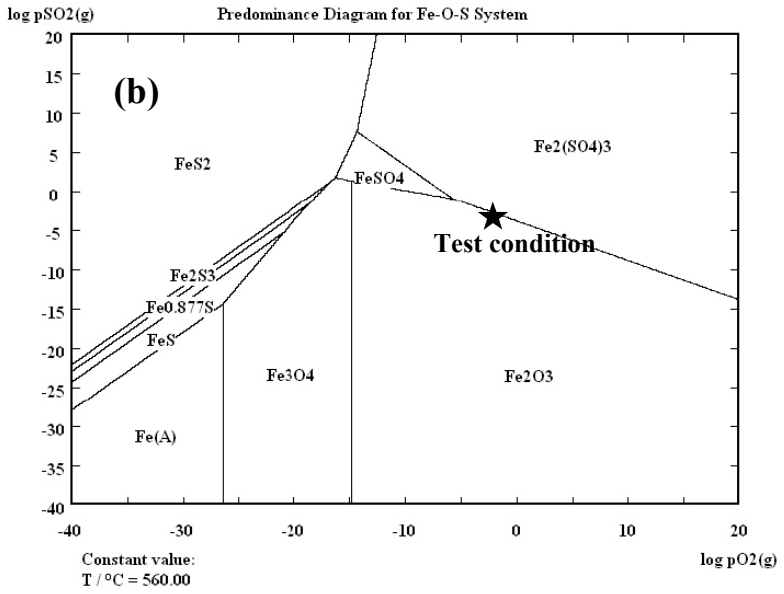

Fig. 5 Thermodynamic stability diagrams of the system at 560^0C (a) Fe-O_2-Cl_2 and (b) Fe-O_2-SO_2

After the removal of the scale, pellet-like oxides were found to cover the whole scale/metal interface (Fig 6a). Since the scale was more porous and its structure was less complete than the scale treated with non HCl-containing gases, the scale/metal interface suffered more S attack. More S was found on the interface in the form of FeS_2/Fe_2S_3/FeS (Fig 6b). Besides, significantly less Cl was found on most of the scale/metal interface due to the high vapor pressure of metal chlorides under this temperature.

Figure 7 is the comparisons of different elements on the surfaces of scales treated with/without HCl gas. In both tests Fe concentrations increased when metal temperatures increased, while O and S concentrations decreased. Regarding the HCl effect on the elementary composition, more porous scales were created by more severe corrosion attack due to the higher HCl concentration where S and Cl were easier to penetrate and reacted with Fe on the metal/scale interface. This was concluded from the results that Fe concentrations from the surfaces of scales with 1000ppm HCl gases were lower than that from the scales without HCl gases.

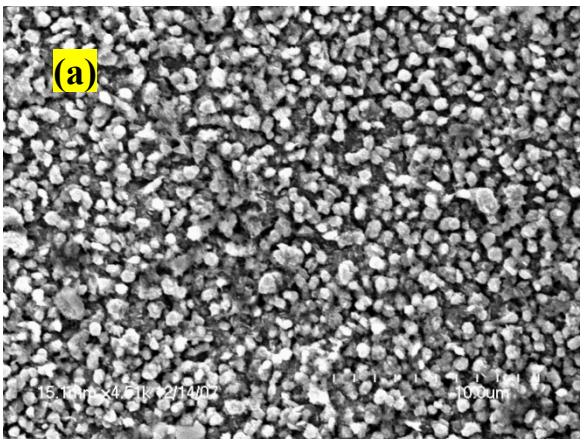

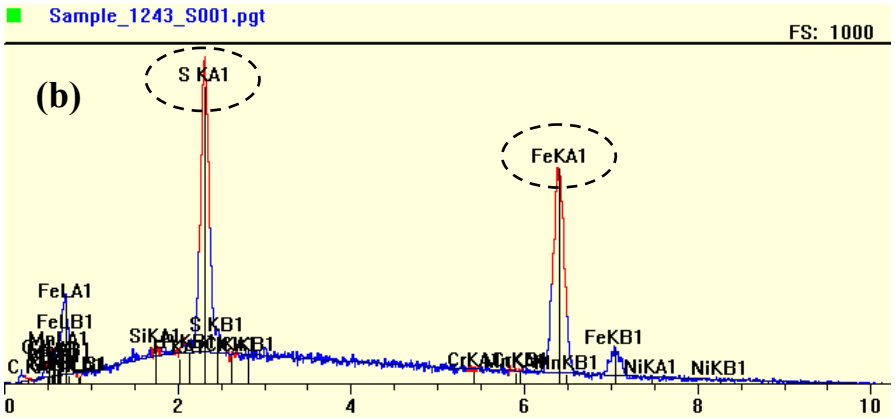

Fig. 6 (a) SEM images of the scale/metal interface after removal of the scale, and (b) Elementary analysis of the scale/metal interface

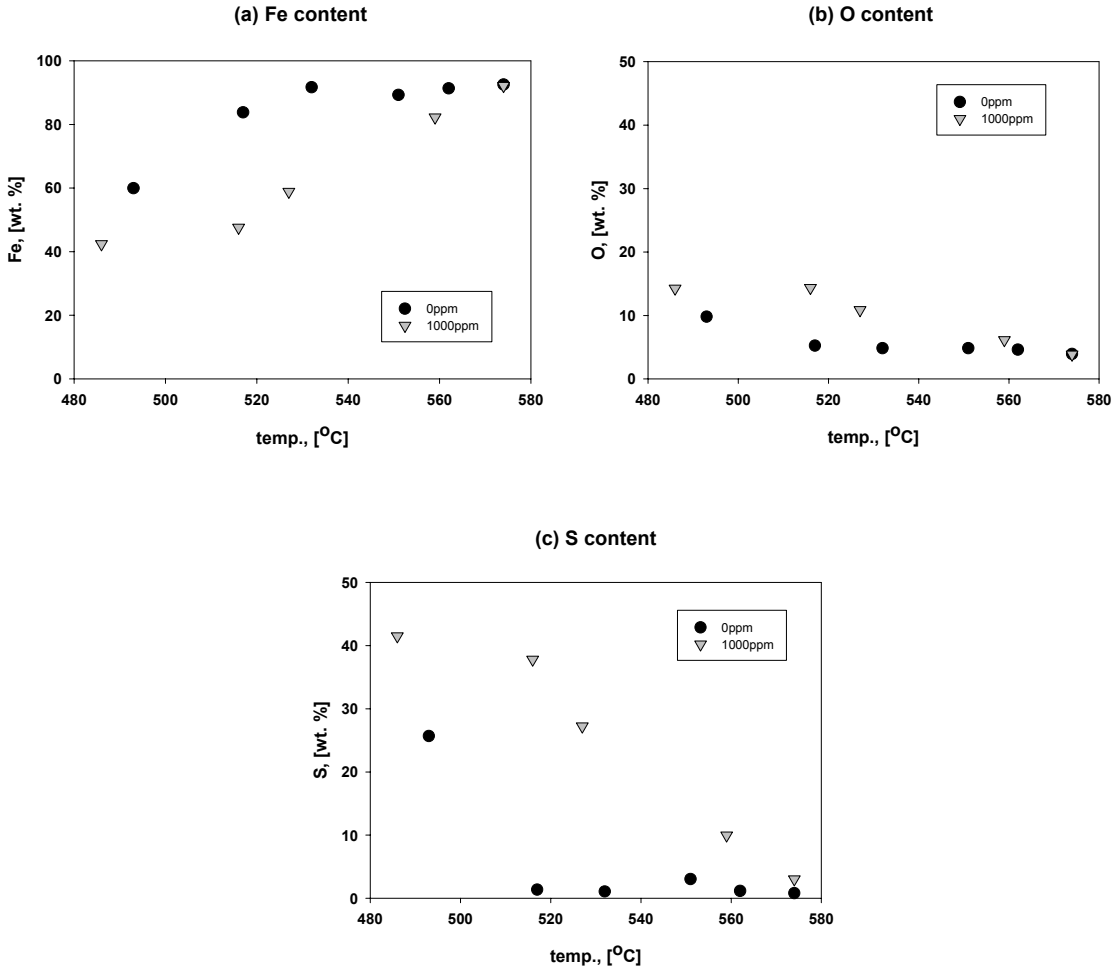

Fig. 7 Elementary analyses of the scales' surfaces; (a) Fe, (b) O, and (c) S

Figure 8 shows the comparison of mass loss corrosion rates with different HCl concentrations. The corrosion rates varied from 10 to 110mills/yr within the range of testing metal temperatures. Higher HCl concentration caused more corrosion, but its relation with corrosion rate was not linear. The corrosion rate increased more when HCl increased from 0 to 500ppm than increased from 500 to 1000ppm. Besides, in all three tests, the higher the metal temperature the higher the corrosion rates were. In the tests with HCl gases, corrosion rates increased dramatically when metal temperatures were higher than 560^0C.

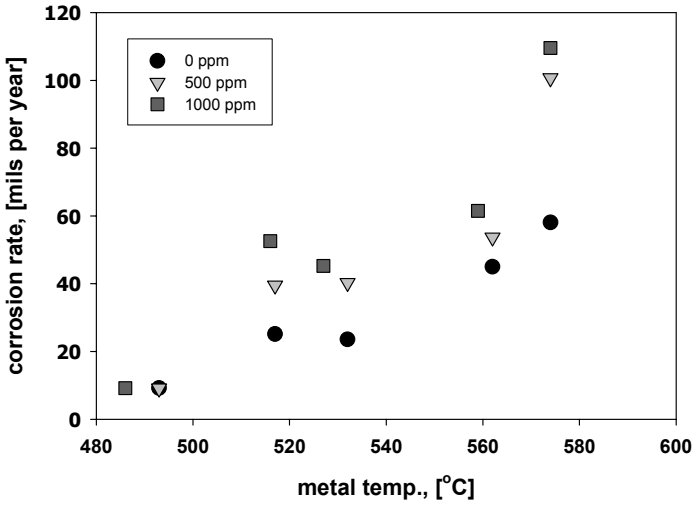

Fig.8 Comparison of mass loss corrosion rates

2. SA213 T11

Figure 9a is the image of the sample after the 100 hrs test with metal temperature of 570^0C and non HCl-containing gases. The whole metal surface was covered by black-reddish scale which was found very porous and consisted of needle-like oxide whiskers under SEM (Fig. 9b). These oxide whiskers rich in Fe and O with a small amount of S were expected to be Fe_2O_3 /$Fe_2(SO_4)_3$ (Fig. 9c).

Figure 10a is the SEM image of the same sample after the removal of the scale from the surface. The scale/metal interface was porous and contained some cracks. EDS results showed high Fe and Cr contents which were different from the scale, but the S content was at about the same level (Fig. 10b). The interface was expected to consist of $Cr_2(SO_4)_3/Cr_2O_3$ and $Fe_2O_3/Fe_2(SO_4)_3$. Compared to the results of SA178A, the addition of Cr element to SA213 T11 protected the metal from being further corroded by S.

Figure 11a is the image of the sample after the 100 hrs test with metal temperature of 565^0C and 1000ppm HCl-containing gases. A grey-reddish thick scale has grown on the sample's surface and suffered from severe spallation when cooled down. Unlike the scale with non HCl treatment, this scale showed some congregate cubic crystals (Fig. 11b). These crystals were rich in Fe, O and S (Fig. 11c). A small amount of Cr was identified. These crystals were expected to be $Fe_2O_3/Fe_2(SO_4)_3$ and $Cr_2(SO_4)_3/Cr_2O_3$.

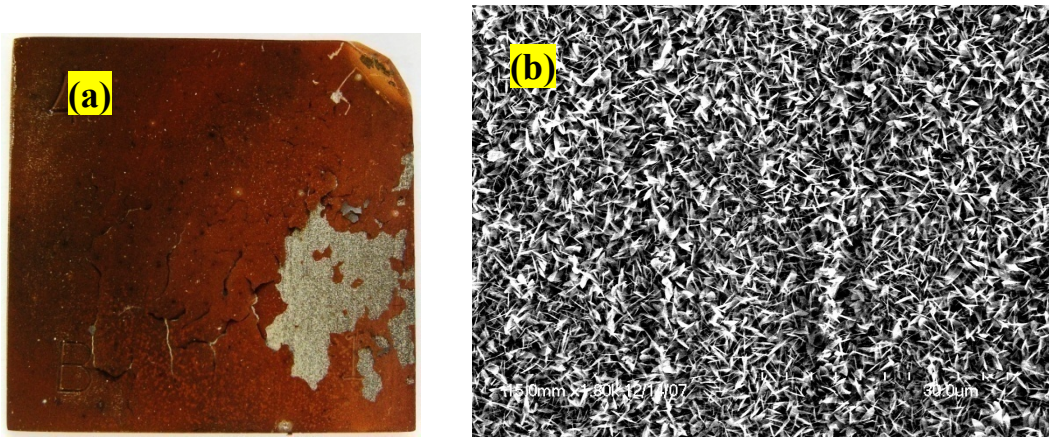

Fig. 9 (a) Surface morphology of sample SA213 T11 tested with non HCl-containing gases, (b) SEM images of the scale, and (c) Elementary analysis of the scale

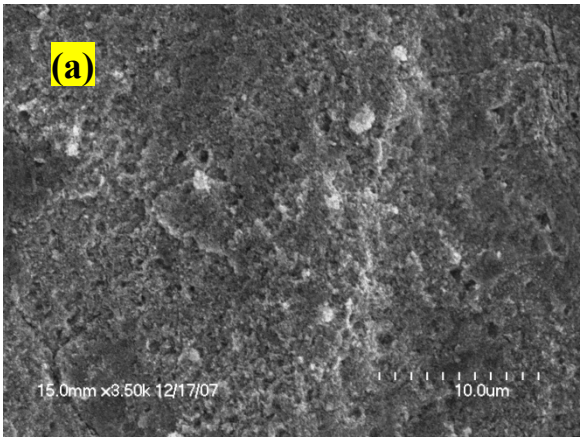

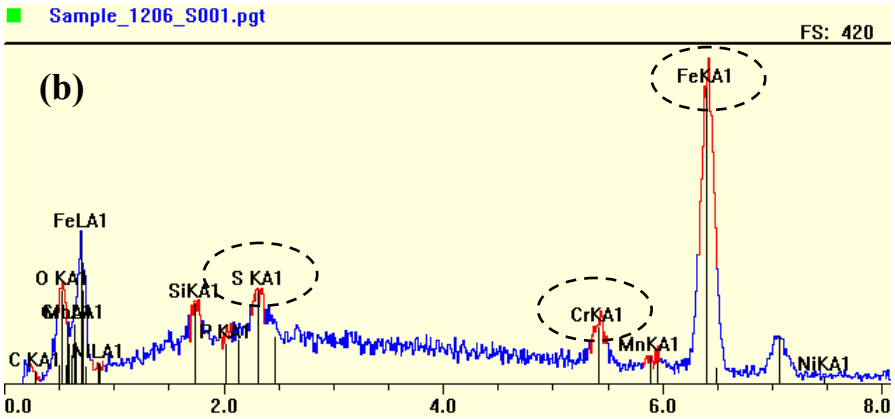

Fig. 10 (a) SEM images of the scale/metal interface after removal of the scale, and (b) Elementary analysis of the scale/metal interface

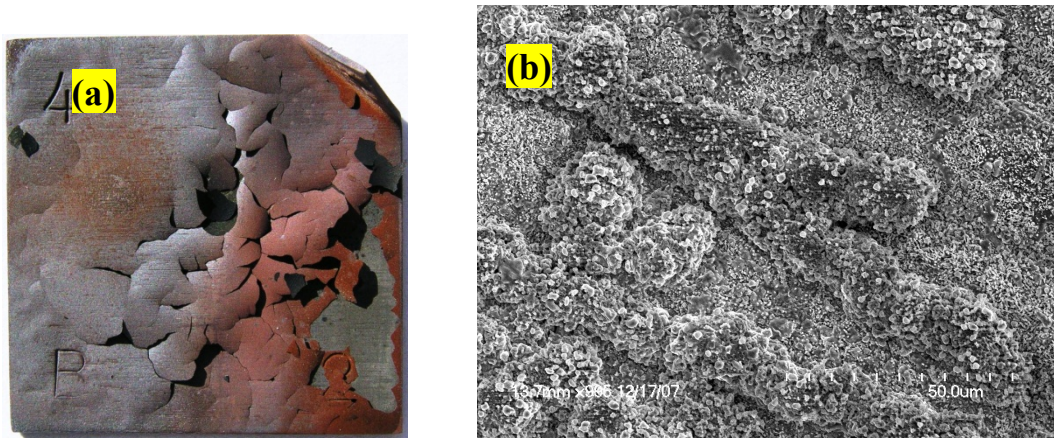

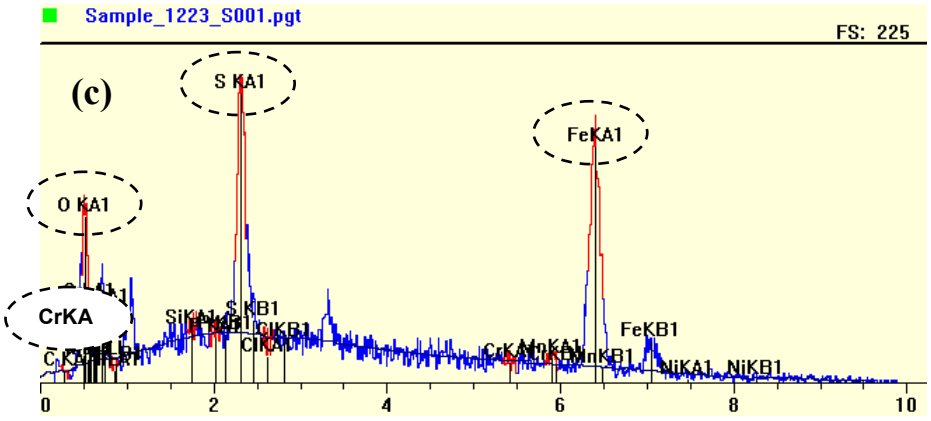

Fig. 11 (a) Surface morphology of sample SA213 T11 tested with 1000ppm HCl-containing gases, (b) SEM images of the scale, and (c) Elementary analysis of the scale

Figure 12a is the SEM image of the same sample after removing the scale on top of the surface. The scale/metal interface was porous and covered unevenly by congregate oxides. The element composition was rich in Fe, Cr and S, but the S content was slightly lower than that in the scale (Fig. 12b). The protection by Cr_2O_3 was less successful due to the Cl attack.

Figure 13 is the comparisons of different elements on the surfaces of scales treated with/without HCl gas. The trends of Fe, O, and S were similar to that shown in sample SA178A except the concentration differences were smaller. The formation of Cr_2O_3 at the initial corrosion stages offered protection of the metal against subsequent S and Cl attacks.

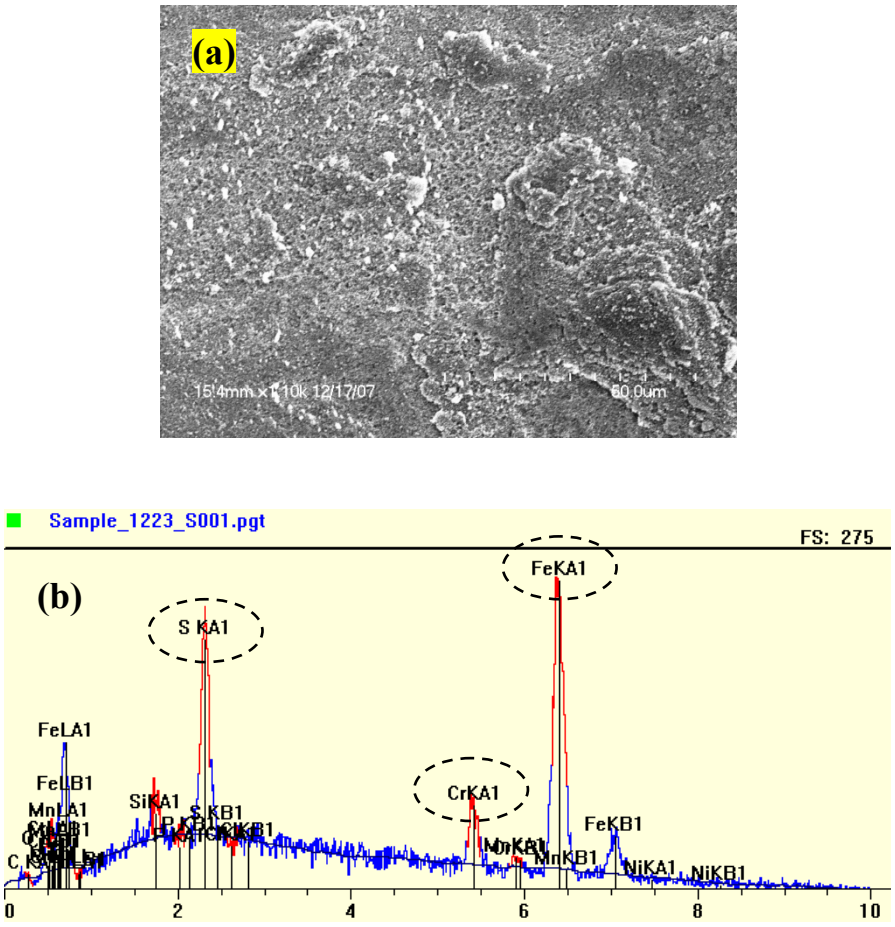

Fig. 12 (a) SEM images of the scale/metal interface after removal of the scale, and (b) Elementary analysis of the scale/metal interface

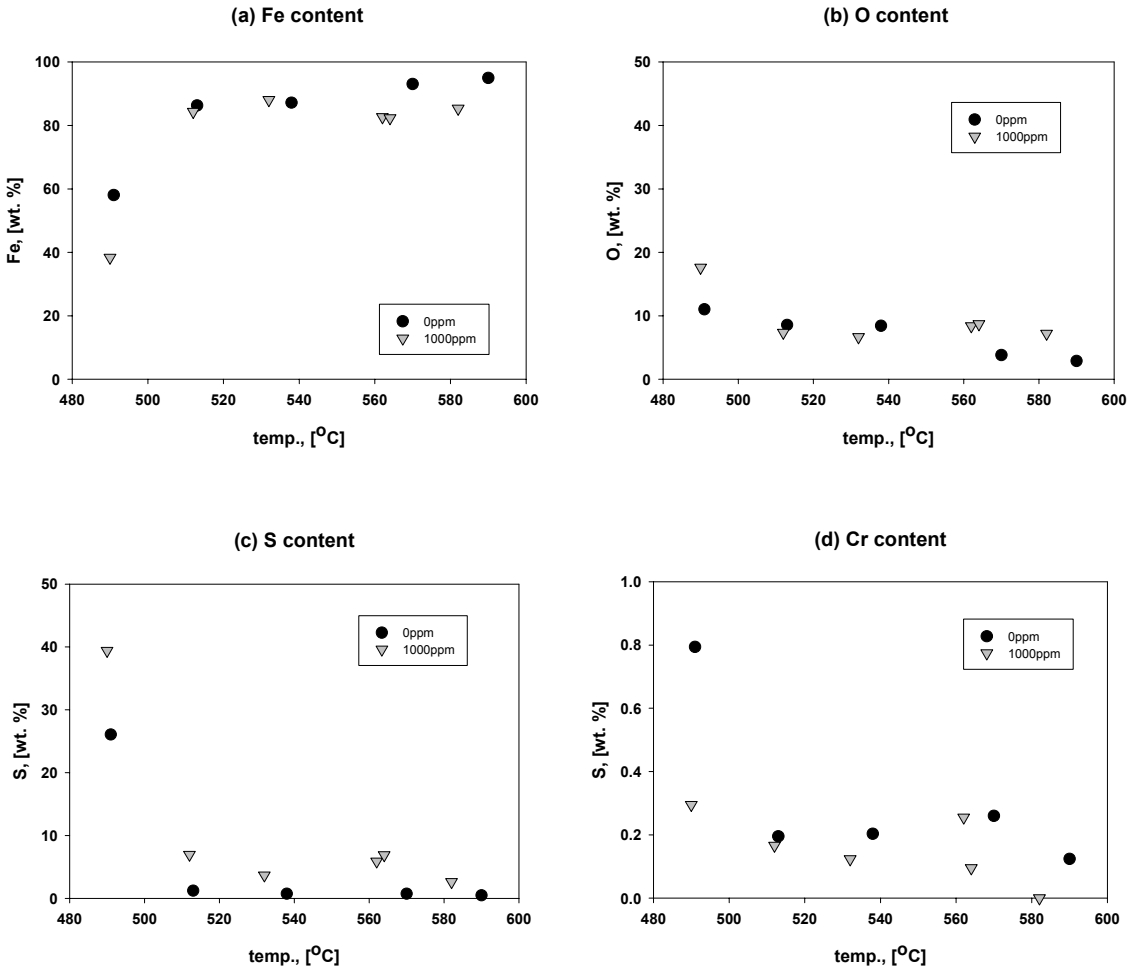

Fig. 13 Elementary analyses of the scales' surfaces; (a) Fe, (b) O, (c) S and (d) Cr

Figure 14 shows the comparison of mass loss corrosion rates with different HCl concentrations. The corrosion rates varied from 15 to 76mills/yr within the range of testing metal temperatures. HCl showed the effect on increasing the corrosion rate, but similar to sample 178A, the relation of corrosion rate and HCl concentration was not linear. The HCl effects were more noticeable when the metal temperature was higher than 560^0C.

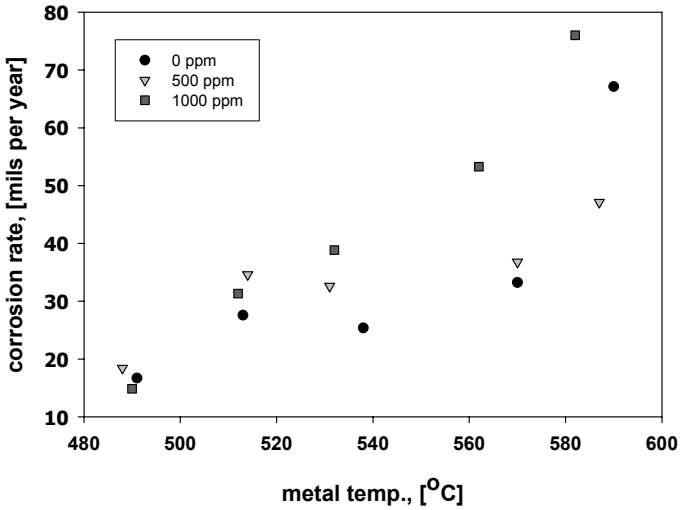

Fig.14 Comparison of mass loss corrosion rates

3. NSSER-4

Fig. 15a shows that the sample retained almost its original surface after the 100 hrs test with metal temperature of 575^{0}C and non HCl-containing gases. The SEM image shows that only a few spots of oxide were deposited on the surface. Except the sample's original elementary composition, O and S were indentified (Fig. 15b and 15c).

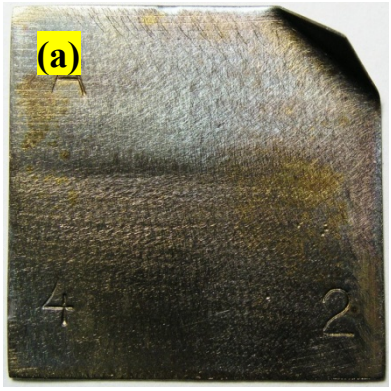

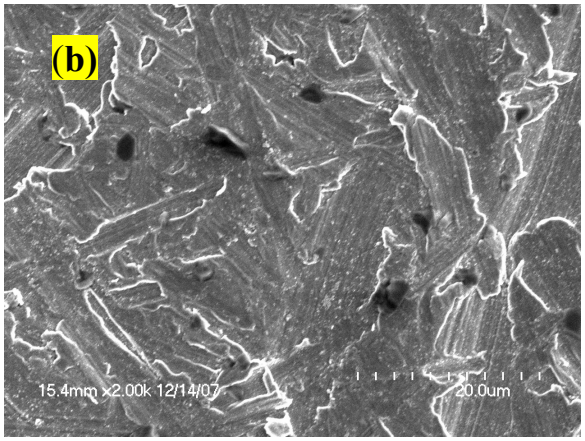

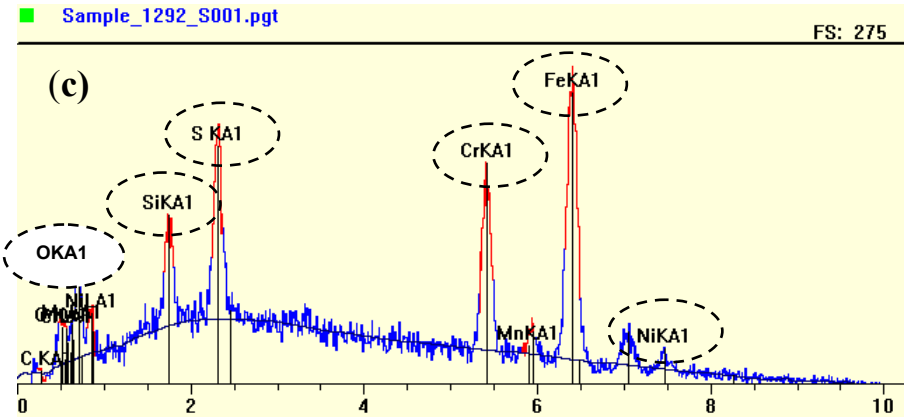

Fig. 15 (a) Surface morphology of sample NSSER-4 tested with non HCl-containing gases, (b) SEM images of the scale, and (c) Elementary analysis of the scale

The appearance of the sample tested with 1000ppm HCl-containing gases was similar to the sample without HCl attacks (Fig. 16a), but SEM image shows that many granular crystals which were in rich in S were deposited over the all surface (Fig. 16b and 16c). The thermodynamic calculations indicated that the compounds were mainly Fe_2O_3, $Fe_2(SO_4)_3$, $NiSO_4$, NiO and Cr_2O_3.

Figure 17 are the comparisons of different elements on the surfaces of scales treated with/without HCl gas. The trends of Fe, O, S and Cr were similar to that shown in sample SA213 T11. The results showed that the formation of NiO and Cr_2O_3 during the corrosion process protected the metal against subsequent S and Cl attacks.

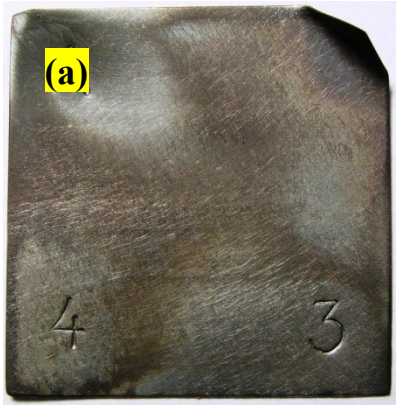

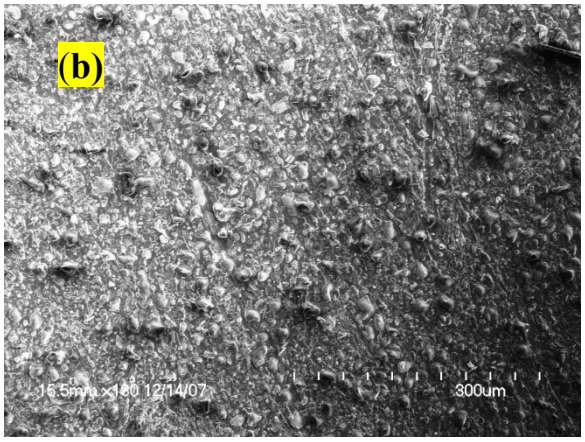

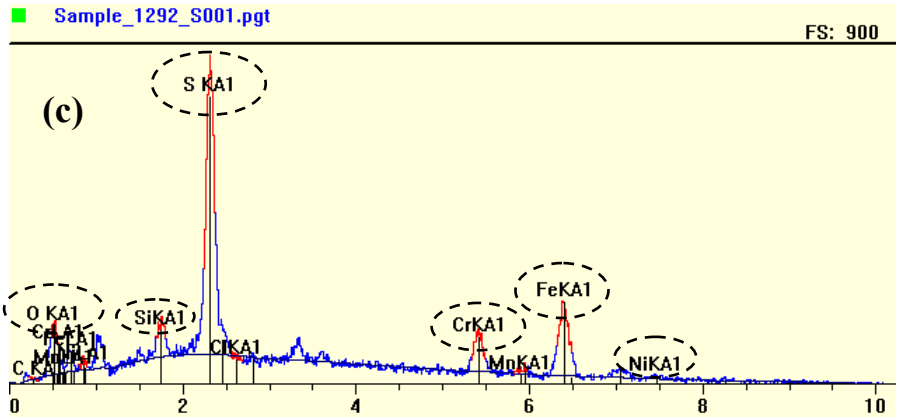

Fig. 16 (a) Surface morphology of sample NSSER-4 tested with 1000ppm HCl-containing gases, (b) SEM images of the scale, and (c) Elementary analysis of the scale

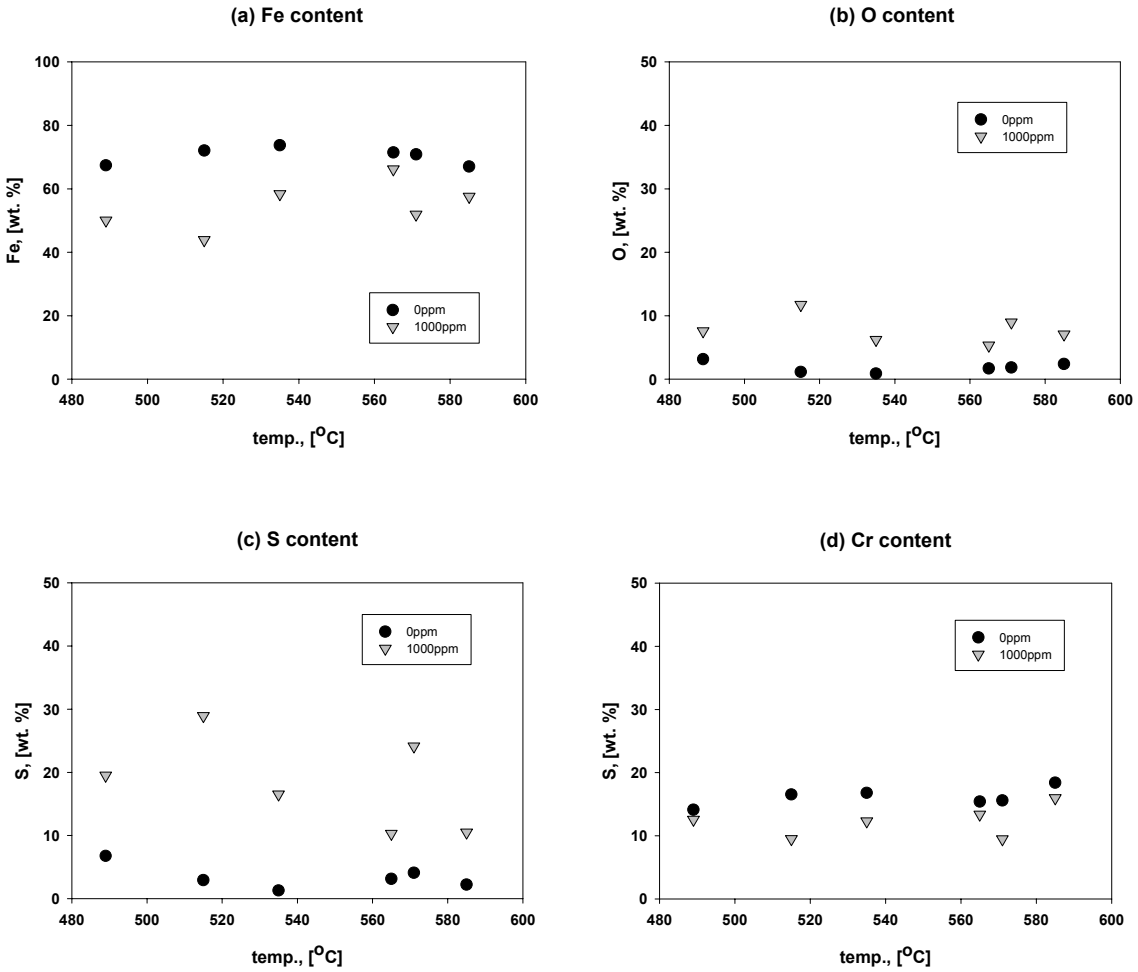

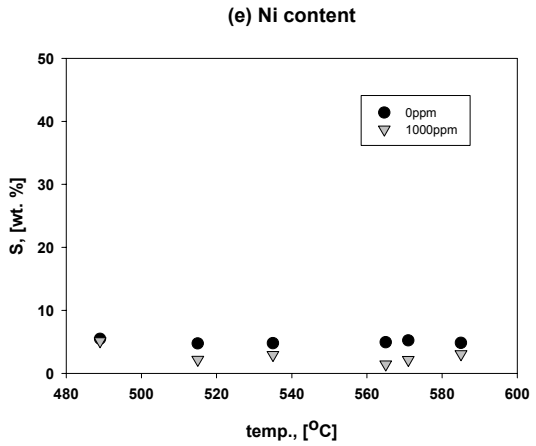

Fig. 17 Elementary analyses of the scales' surfaces; (a) Fe, (b) O, (c) S, (d) Cr, and (e) Ni

NSSER-4 showed a good corrosion resistance (under 3.0 mills/yr) within the temperature range of 480^0C -580^0C (Fig. 18). The addition of HCl gas increased the corrosion rate especially from 0 to 500ppm. When the metal temperature was over 580^0C, corrosion rates increased dramatically and the effect of HCl gas was also magnified.

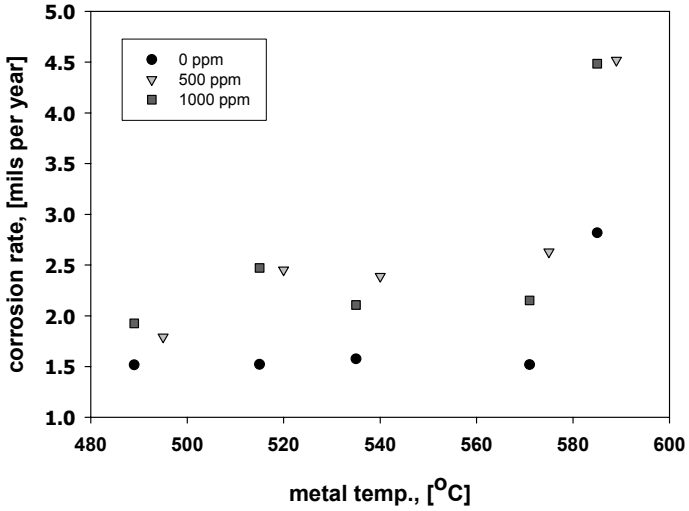

Fig.18 Comparison of mass loss corrosion rates

CONCLUSIONS

The addition of 500 and 1000ppm HCl to the synthetic gas increased the corrosion rates of these three test samples, although the relation between the HCl concentration and corrosion rate was not linear. The HCl effects on corrosion rates were more prominent when its concentration changed from 0 to 500ppm. In addition, the HCl effects were promoted by the increase of metal temperature. When the metal

temperature was below 500^0C, HCl effect was negligible, while its effect increased significantly when the metal temperature was over 560^0C.

In order to simulate the gas environment in the WTE facility, another corrosive gas - SO_2 was included in the synthetic gas in addition to HCl. The advantage of this approach was that the corrosion rates acquired from the test could reflect the practical situations in WTE facilities. On the other hand, this also increased the complex of analyzing the corrosion resistance of different elements in a sample and the difficulty of isolating the HCl effect from the overall corrosion rate.

ACKNOWLEDGEMENT

The authors gratefully acknowledge the assistance of Prof. Paul F. Duby (Department of Earth and Engineering at Columbia University) and Prof. Cevdet Noyan for lending the lab space.

REFERENCES

1. Albina, D.O., Theory and experience on corrosion of waterwall and superheater tubes of Waste-To-Energy facilities, in Department of Earth and Environmental Engineering. 2005, Columbia University.
2. Themelis, N.J., *Chlorine Balance in a Waste-To-Energy Facility*. 2005, Earth Engineering Center.
3. A. Zahs, M.S.H.G., The influence of alloying elements on the chlorine-induced high temperature corrosion of Fe-Cr alloys in oxidizing atmospheres. Materials and Corrosion, 1999. **50**(10): p. 561-578.
4. Kawahara, Y., Evaluation of high-temperature corrosion life using temperature gradient corrosion test with thermal cycle component in waste combustion environments. Materials and Corrosion, 2006. **57**(1): p. 60-72.
5. Stott, F.H. and C.Y. Shih, *The influence of HCl on the oxidation of iron at elevated temperatures.* Materials and Corrosion, 2000. **51**(5): p. 277-286.
6. Asteman, H. and M. Spiegel, Investigation of the HCl (g) attack on pre-oxidized pure Fe, Cr, Ni and commercial 304 steel at 400 [degree sign]C. Corrosion Science, 2007. **49**(9): p. 3626-3637.
7. Persson, K., et al., *High temperature corrosion in a 65 MW waste to energy plant.* Fuel Processing Technology, 2007. **88**(11-12): p. 1178-1182.
8. Grabke, H.J., E. Reese, and M. Spiegel, The effects of chlorides, hydrogen chloride, and sulfur dioxide in the oxidation of steels below deposits. Corrosion Science, 1995. **37**(7): p. 1023-1043.
9. Lee, S.-H. and M.J. Castaldi, High temperature corrosion resistance of different commercial alloys under various corrosive environments, in The North American Waste-to-Energy Conference 2007: Miami, FL.